

# Recent Developments for the SINFONI Pipeline

Konstantin Mirny<sup>a</sup>, Andrea Modigliani<sup>b</sup>, Mark J. Neeser<sup>b</sup> and Dieter Nürnberger<sup>c</sup>

<sup>a</sup>Radius Z, Bunsenstr 24, München, Germany;

<sup>b</sup>European Southern Observatory, Karl Schwarzschild Str. 2, Garching, Germany;

<sup>c</sup>European Southern Observatory, Alonso de Cordova 3107 Vitacura, Santiago, Chile.

## ABSTRACT

The SINFONI data reduction pipeline, as part of the ESO-VLT Data Flow System, includes recipes for Paranal Science Operations, and for Data Flow Operations at Garching headquarters. At Paranal, it is used for the quick-look data evaluation. The pipeline is available to the science community for reprocessing data with personalised reduction strategies and parameters. The recipes are implemented with the ESO Common Pipeline Library (CPL). SINFONI is the Spectrograph for INtegral Field Observations in the Near Infrared (1.1-2.45  $\mu\text{m}$ ) at the ESO-VLT, and was developed and built by ESO and MPE in collaboration with NOVA. It consists of the SPIFFI (SPectrometer for Infrared Faint Field Imaging) integral field spectrograph and an adaptive optics module which allows point spread functions very close to the diffraction limit. The image slicer of SPIFFI chops the SINFONI field of view on the sky into 32 slices which are re-arranged to a pseudo slit. The latter is then dispersed by one of four possible gratings (J, H, K, and H+K). The instrument thus produces a two-dimensional (2D) raw image that contains both spatial (along the pseudo-slit) and spectral information. The ultimate task of the SINFONI pipeline is to reconstruct this frame into a three-dimensional (3D) data cube, with the x and y axes representing the spatial, on-sky dimension, and the corresponding spectrum of each spatial pixel along the z-axis.

In the present article we describe two major improvements to the SINFONI pipeline. The first is a development to monitor instrument efficiency and stellar zero-points using telluric standard stars. The second involves the implementation of a semi-empirical algorithm to calibrate and remove the effects of atmospheric refraction, sometimes visible in the 3D cube reconstruction. The latter improves the positional offsets through the wavelength cube to an r.m.s. shift of better than 0.25 pixels.

**Keywords:** Astronomical Data Reduction, IFU cube reconstruction

## 1. INTRODUCTION

The Pipeline Systems Department of the Software Development Division at ESO is responsible for the development of instrument data reduction pipelines,<sup>1,2</sup> The pipelines are used by Paranal and La Silla operations as quick-look tools to do a real-time coarse assessment of the quality of calibrations and science observations. When the data arrive at ESO Garching (generally within one hour), a more thorough data processing and evaluation is performed by the Quality Control group. Here, the pipeline is used to automatically process raw calibration frames into master calibrations, generate quality control parameters in order to monitor the telescope, instrument, and detector performance, and to assess the quality of the calibrations and science observations. Finally, the pipelines are also released to the public to allow any instrument or archive user to do a data reduction optimized to their science case.

The VLT instrument pipeline releases are publicly available at [www.eso.org/pipelines](http://www.eso.org/pipelines). The results of the SINFONI data quality control<sup>3</sup> are deployed at [www.eso.org/observing/dfo/quality/SINFONI/qc/qc1.html](http://www.eso.org/observing/dfo/quality/SINFONI/qc/qc1.html)

SINFONI is the Spectrograph for INtegral Field Observations in the Near Infrared (1.1-2.45  $\mu\text{m}$ ) at the VLT,<sup>4,5</sup>

We present two major improvements in the SINFONI data reduction pipeline.

---

Further author information: (Send correspondence to K.M. and A.M.)

K.M.: E-mail: [kmirny@eso.org](mailto:kmirny@eso.org), Telephone: +49 (0)89 320 06 879

A.M.: E-mail: [amodigli@eso.org](mailto:amodigli@eso.org), Telephone: +49 (0)89 320 06 789

Observatory Operations: Strategies, Processes, and Systems III, edited by  
David R. Silva, Alison B. Peck, B. Thomas Soifer, Proc. of SPIE Vol. 7737, 77371R  
© 2010 SPIE · CCC code: 0277-786X/10/\$18 · doi: 10.1117/12.856961

The first is an important part of the instrument performance quality control and consists of the continuous monitoring of the efficiency and stellar zero-points using telluric standard stars. We briefly describe the implemented algorithm and provide preliminary results.

The second involves an improvement to the main science data reduction product of the SINFONI pipeline: the 3D data cube. This pipeline product provides both spatial and spectral information with each plane of the cube as a monochromatic image of the SINFONI field of view, and the cube z-axis spanning the SINFONI spectrograph wavelength range in one of the observing bands J, H, K, or H+K. We have found that differential atmospheric refraction can introduce a wavelength dependency in the object position that can affect the quality of the reconstructed cube. This is most evident in the waveband having the largest wavelength span (H+K) and at the camera setting with the smallest pixel scales (25 mas).

A semi-empirical correction procedure based on telluric standard star data sets spanning five years of SINFONI operations, allows us to reduce measured positional shifts in the data cube (sometimes as large as 12 pixels) to a fraction of a pixel.

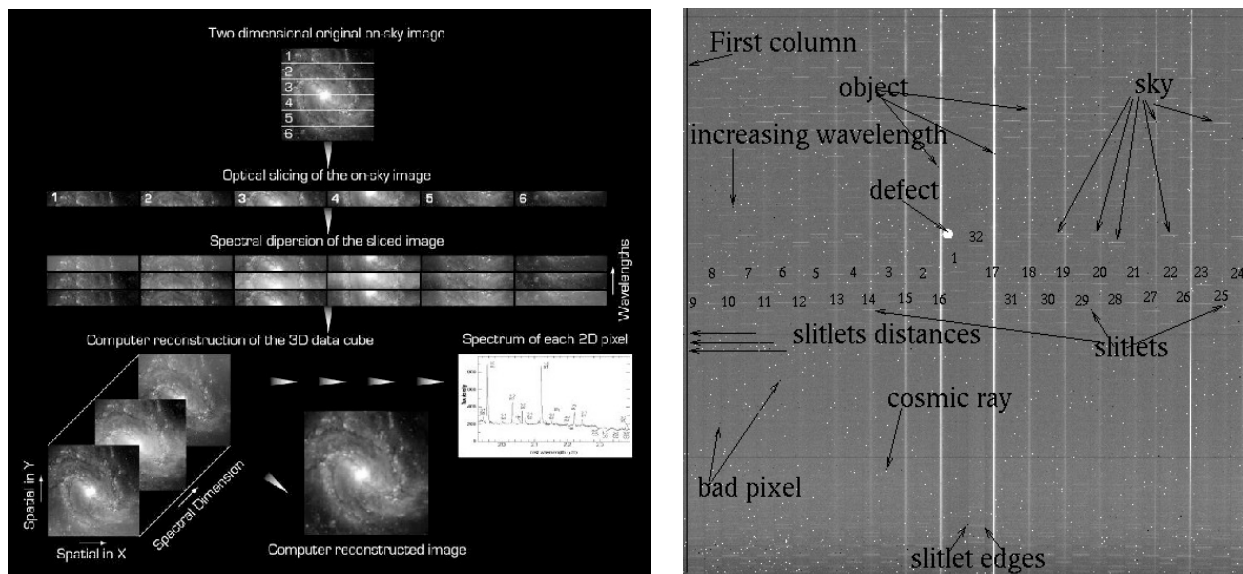


Figure 1. A simplified schematic of the principle of IFU data and the main data reduction steps needed for image reconstruction (left hand panel). An annotated SINFONI science raw frame (right hand panel).

## 2. THE SINFONI PIPELINE DATA REDUCTION IN A NUTSHELL

This section provides a summary description of the data reduction steps required to build a calibrated science 3D data cube.<sup>6</sup>

The SINFONI field of view is sliced into 32 elements by the image slicer, collected as a pseudo-slit on the entrance slit to the spectrometer and then dispersed and imaged in a brick wall pattern on the NIR detector array. The spatial coordinate is given along the X direction and the wavelength dispersion is along the Y direction. Fig. 1 provides a simplified schematic description of the IFU functionality and main data reduction steps (left hand panel) and an image of an annotated science raw frame (right hand panel).

The pipeline is used to reconstruct the SINFONI field of view from the complex 32 slices spectra, once the instrument signature has been corrected.

The intrinsic detector emission at zero integration time is removed by taking calibration exposures in a sequence of lamp-on and lamp-off exposures and subtracting them in on-off pairs.

The pipeline measures the instrument optical distortions by processing several frames obtained by illuminating all of the IFU slices with a calibration fibre that is moved along the instrument's North-South direction. As the

fibre can illuminate only a few slices in a non-uniform way, more than 70 individual frames need to be combined to build a synthetic image that contains well-exposed continuum spectrum traces in each slice. After detecting the Gaussian peak of the fibre trace in the spectrum of the detector, the pipeline builds a grid of equi-distant points along vertical traces centered at the peak flux positions. The pipeline then computes a two-dimensional polynomial transformation that maps each detector position in the distorted frame to the corresponding one in the distortion-corrected space.

Following dark frame subtraction, master flat, distortion and bad pixel correction, the pipeline uses a simple linear model, and the lab-measured dispersion values in the observed band setting to determine the approximate Y position of spectral emission features in the calibration arc lamp frame. Convoluting the predicted line position with a Gaussian of a given FWHM and intensity, a synthetic arc line spectrum is computed that can then be fit to the actual calibration frame. A non-linear least-square fit is made to each emission line along the dispersion axis of the image, resulting in a line amplitude, centroid, FWHM, and background level for each  $(x, y, \lambda)$ . A low-order, 2D polynomial fit is then made along the spatial direction in order to remove spurious outliers that may have occurred during the line detection. Finally the pipeline generates a 2D wavelength map in which each image pixel is given an intensity equal to the corresponding calibrated wavelength. The wavelength calibration frame is also used to locate and trace the slitlet edges that is later used to reconstruct the instrument field of view.

Science frame data reduction pass through the following steps. The object and sky frames are both corrected for dark current emission, and the sky frame is then subtracted from the object frame. The resulting image is flat-fielded using the master lamp flat and the distortion and bad pixel corrections are applied. Using the 2D wavelength dispersion solution, the images are re-sampled from their original spatial-spatial form into a spatial-wavelength format. Finally, using the information of the image slicing pattern fixed on the detector and the calibrated edges of each of the traces, the spatial information contained in each of the 32 slices is re-assembled into a 64x64 pixel image for each of roughly 2200 wavelength steps. This final product is a 3D data cube with the instrument field of view (x,y) given at each wavelength (z).

In case of an observation is composed of a sequence of target object frames a cube for each object frame is generated. Finally the pipeline uses the WCS information contained in the FITS header to combine the cubes into a single cube mosaic.

### 3. EFFICIENCY DETERMINATION

For SINFONI observations of telluric standard stars, it is possible to use the sky-background corrected standard star spectrum, to estimate the instrument efficiency (i.e. the combined throughput of the atmosphere, telescope, and instrument).

The efficiency at a given wavelength  $\lambda$  is computed as:

$$\epsilon(\lambda) = \frac{S(\lambda) \cdot 10^{0.4 \cdot \text{Atm\_ext}(\lambda) \cdot (\text{airp} - \text{airm}) \cdot G \cdot E_{\text{phot}}(\lambda)}{T_{\text{exp}} \cdot A_{\text{tel}} \cdot R(\lambda)} \cdot F$$

Where  $S(\lambda)$  is the extracted standard star spectrum as observed with SINFONI, corrected for the contribution from the sky background, at a given wavelength  $\lambda$ .  $\text{Atm\_ext}(\lambda)$  is the value of the atmospheric extinction,  $\text{airm}$  is the airmass at which the star was observed, and  $\text{airp}$  is a parameter to indicate if the efficiency is be computed at airmass=0 (no-atmosphere) or at a given value (usually the one at which the reference standard star spectrum has been tabulated). The  $G$  is the detector gain ( $e^{-1}/ADU$ ),  $E_{\text{phot}}(\lambda)$  is the energy of a single input photon ( $E_{\text{phot}}(\lambda) = \frac{10^7}{\lambda \cdot 1.986 \cdot 10^{19}} \text{ J } \mu\text{m}^{-1}$ ),  $T_{\text{exp}}$  is the total exposure time in seconds,  $A_{\text{tel}}$  is the telescope collecting area (for the VLT UT's this is  $51.2 \cdot 10^4 \text{ cm}^2$ ),  $R(\lambda)$  is the flux calibrated spectrum of the reference source, and  $F$  is a multiplicative factor that corrects for the fact that the above formula contains terms that have been expressed in different units.

Since telluric standards are typically observed several times per night, monitoring their efficiency in known or uniform atmospheric conditions, can give a deep insight into the health of the instrument.

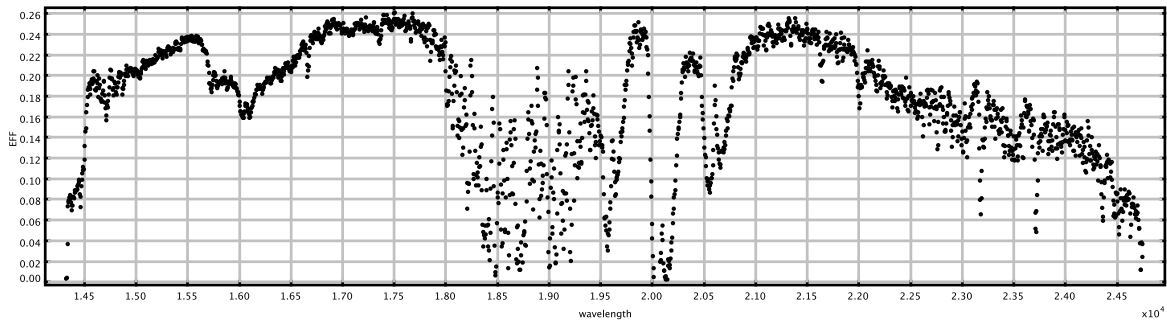


Figure 2. SINFONI efficiency as measured with the telluric standard star BD+17-4708 (H+K band at the 250 mas pixel scale).

#### 4. ATMOSPHERIC REFRACTION CALIBRATION AND CORRECTION

During SINFONI operations we have found cases in which the centroid position of an observed source systematically shifts by several pixels as a function of wavelength.

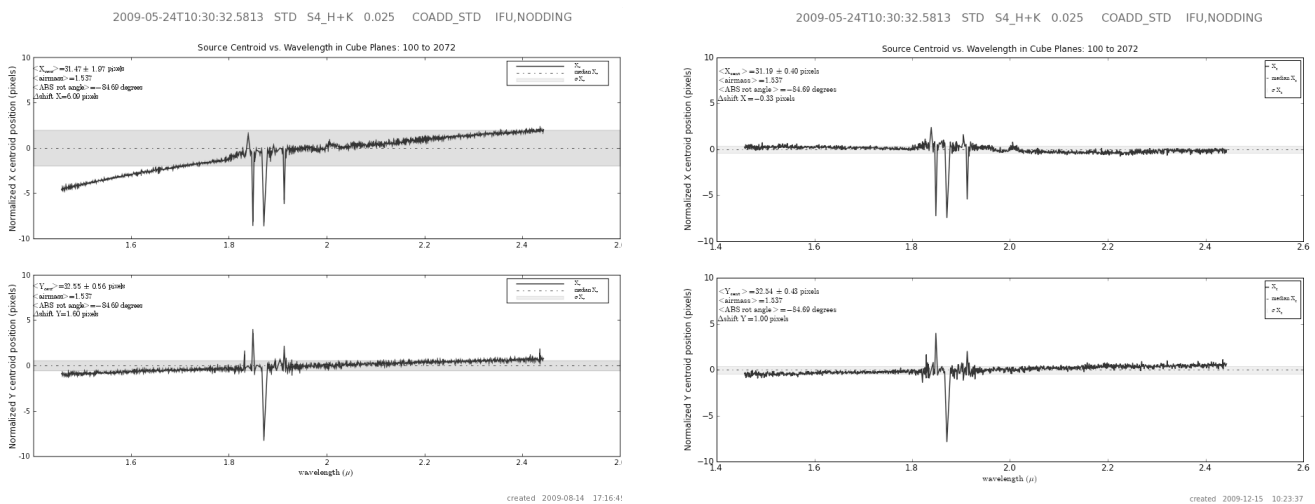


Figure 3. A trace through the data cubes of the telluric standard star is shown. The panels show the normalized X- (top) and Y-axis (bottom) centroid positions of the standard star as a function of wavelength through the data cube. The right panel has been corrected for atmospheric refraction, while the left hand panel has not.

A typical example of this is shown in left panel of Fig. 3, where we have plotted a trace of the centroid of a bright standard star through its data cube. This effect is particularly noticeable when using the grism with the largest wavelength range (i.e. the H+K band covering 1.45 to 2.45  $\mu\text{m}$ ) at the finest spatial scale (i.e. 25 mas). At the largest spatial setting available for SINFONI (250 mas) this effect becomes negligible.

In order to monitor the image quality and the adaptive optics performance, an illuminated internal fibre is imaged as part of SINFONI's daily health checks. The drift in the centroid position as a function of wavelength is entirely absent in the data cubes created for the internal fibre. This confirms that the centroid shifts cannot be explained by some error in the data reduction itself, but must arise outside of the instrument and pipeline. An obvious culprit, better known at much bluer optical wavebands, is atmospheric refraction. Due to variations

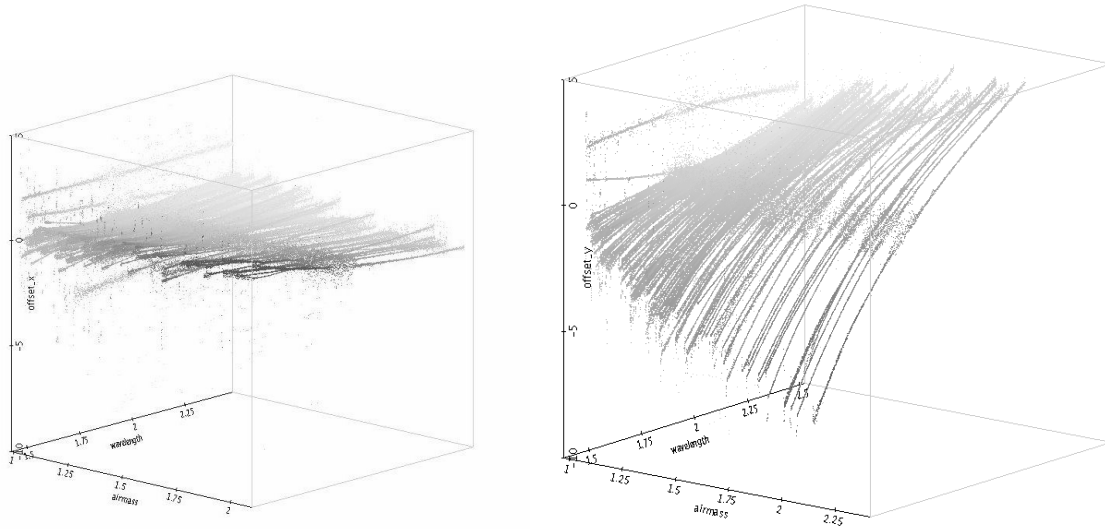


Figure 4. Measured offsets along the east-west (left hand panel) and north-south (right hand panel) directions as a function of wavelength for a range of airmasses (H+K band at the 25 mas pixel scale). Clearly, the north-south axis has the largest refractive offsets with the largest airmass values producing shifts of up to 12 pixels.

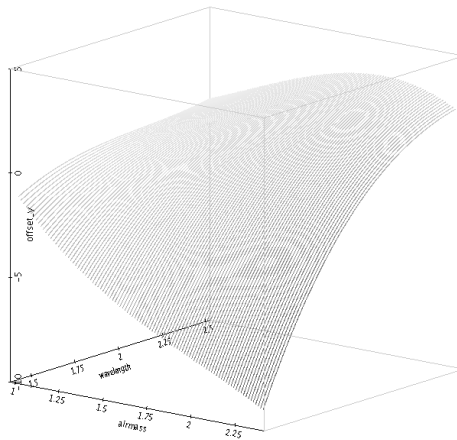


Figure 5. A  $3^{rd}$  order polynomial surface (for the H+K band at 25 mas) derived from the centroid offsets measured in thousands of standard star cubes. We use polynomial coefficients of this surface to correct the any data cube of its atmospheric refraction offset based on its airmass value.

in air density as a function of altitude and the bending of light rays through this medium, an object's position on the focal plane will depend on its wavelength and the airmass of its observation.

We initially attempted to apply theoretical atmospheric refraction models to the SINFONI data, but found that the results where not satisfying.

A detailed study of this problem using SINFONI standard stars has shown a clear dependency of the centroid shift on airmass and wavelength. As the airmass is a function of the zenith distance, and as each SINFONI observation is generally performed with a different orientation on the sky, we have corrected for the instrument position angle and decomposed the centroid shift in terms of its east-west and north-south components.

Using the several thousand telluric standard star observations obtained during SINFONI's lifetime, we have built up a catalogue of sources matching a wide range of airmasses to the measured centroid shift (corrected for

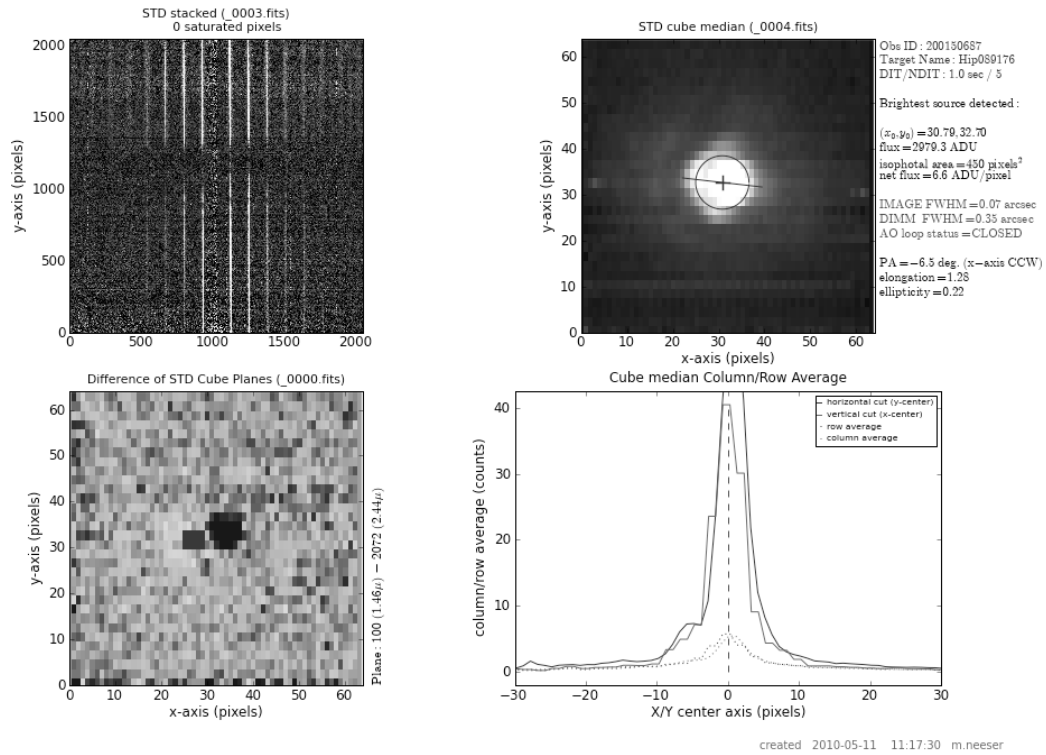


Figure 6. The quality control plots for a SINFONI telluric standard star processed without the atmospheric refraction correction applied to the data cubes. The difference between cube plane 100 and cube plane 2072 (the bottom left frame) best shows the effect of atmospheric refraction as a function of wavelength through a SINFONI data cube. This difference image shows a 6 pixel offset.

the instrument position angle), for each of the observing bands (J, H, K, and H+K) and spatial scales (25, 100, 250 mas).

As expected, the north-south axis has the largest refractive offsets, while the east-west components are well within the measurement noise and show no systematic offsets. Furthermore, the north-south decomposition shows that the largest airmass values producing shifts of up to 12 pixels (for the H+K band at the 25 mas pixel scale). See Fig. 4. The shifts along the north-south direction can be well-defined by a polynomial surface. At the 250 mas pixel scale the offset fluctuations can be neglected as their r.m.s lies within one pixel.

For the 25 and 100 mas pixel scales, a third order polynomial surface fit has been made of the atmospheric refraction shifts as a function of wavelength and airmass. The 25 mas example of this surface is shown in Fig.5. The polynomial fit coefficients are saved in a reference calibration table for each observing band and spatial scale.

When a new object is observed at a given airmass, the pipeline uses the associated polynomial fit coefficients to compute, for each wavelength, the corresponding shift along the north-south direction. This is then converted to x and y-axis shifts using the instrument orientation (as read from the ABSROT START and ABSROT END image keywords), and the corresponding shifts are applied to each plane of the data cube.

The improvement in the reconstructed data cubes can be clearly seen in comparison of the quality control plots of a standard star with and without the atmospheric refraction correction applied (see Fig. 3, 6 and 7).

At the largest observed airmass available in the SINFONI standard star archive we have seen shifts as large as 12 pixels ( $\pm 6$  pixels with respect to the cube center). Using our correction we can always reduce these extreme values to less than  $\pm 1.0$  pixels, but more generally we achieve a correction better than  $\pm 0.25$  pixels.

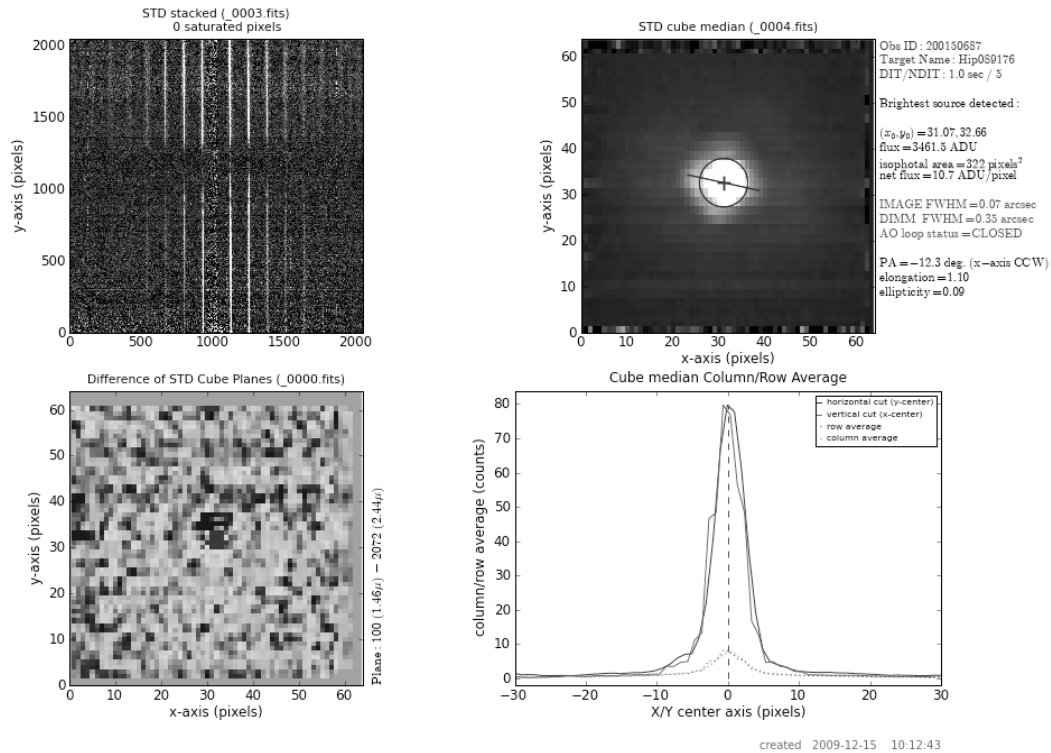


Figure 7. The quality control plots for a SINFONI telluric standard star processed with the atmospheric refraction correction applied to the data cubes. The difference between cube plane 100 and cube plane 2072 (the bottom left frame) best shows the effect of atmospheric refraction as a function of wavelength through a SINFONI data cube. This difference image shows a sub-pixel scale offset when the correction is applied.

## 5. CONCLUSIONS AND SUMMARY

We have presented results on recent developments in the SINFONI pipeline. It is now possible to monitor the cumulative telescope, instrument, and detector efficiencies and to monitor the zero-points of the telluric standard stars.

By implementing a semi-empirical atmospheric refraction model, the SINFONI pipeline now corrects the wavelength shifts in the data cubes and has improved the spatial accuracy to a small fraction of a pixel. By using this correction, the global astrometric accuracy of each plane of the SINFONI data cubes has been greatly increased. This should improve the signal-to-noise of an extracted source spectrum, since a given object aperture can remain fixed throughout the data cube. This will be most evident when extracting the spectra of the faintest sources.

## REFERENCES

- [1] Ballester, P., Banse, K., Castro, S., Hanuschik, R., Hook, R. N., Izzo, C., Jung, Y., Kaufer, A., Larsen, J. M., Licha, T., Lorch, H., Lundin, L., Modigliani, A., Palsa, R., Peron, M., Sabet, C., and Vinther, J., “Data reduction pipelines for the very large telescope,” in [*Observatory Operations: Strategies, Processes, and Systems.*], Silva, D. R.; Doxsey, R. E., ed., *Proc. SPIE* **6270** (2006).
- [2] Silva, D. and Peron, M., “Vlt science products produced by pipelines: A status report,” *The Messenger* **118**, 2 (Dec. 2004).
- [3] Hummel, W., Modigliani, A., Szeifert, T., and Dumas, C., “Data flow operations and quality control of sinfoni,” *New Astronomy Reviews* **50**, 412 (June 2006).

- [4] Bonnet, H., Abuter, R., Baker, A., Bornemann, W., Brown, A., Castillo, R., Conzelmann, R., Damster, R., Davies, R., Delabre, B., Donaldson, R., Dumas, C., Eisenhauer, F., Elswijk, E., Fedrigo, E., Finger, G., Gemperlein, H., Genzel, R., Gilbert, A., Gillet, G., Goldbrunner, A., Horrobin, M., Ter Horst, R., Huber, S., Hubin, N., Iserlohe, C., Kaufer, A., Kissler-Patig, M., Kragt, J., Kroes, G., Lehnert, M., Lieb, W., Liske, J., Lizon, J. L., Lutz, D., Modigliani, A., Monnet, G., Nesvadba, N., Patig, J., Pragt, J., Reunanen, J., Rohrle, C., Rossi, S., Schmutzer, R., Schoenmaker, T., Schreiber, J., Stroebele, S., Szeifert, T., Tacconi, L., Tecza, M., Thatte, N., Tordo, S., van der Werf, P., and Weisz, H., "First light of SINFONI at the VLT," *The Messenger* **117**, 17 (Sept. 2004).
- [5] Eisenhauer, F., Abuter, R., Bickert, K., Biancat-Marchet, F., Bonnet, H., Brynnel, J., Conzelmann, R., Delabre, B., Donaldson, R., Farinato, J., Fedrigo, E., Genzel, R., Hubin, N., Iserlohe, C., Kasper, M., Kissler-Patig, M., Monnet, G., Roehle, C., Schreiber, J., Stroebele, S., Tecza, M., Thatte, N., and Weisz, H., "Sinfoni - integral field spectroscopy at 50 milli-arcsecond resolution with the eso vlt," in [*Instrument Design and Performance for Optical/Infrared Ground-based Telescopes.*], I. Masanori; Moorwood, Alan F. M., ed., *Proc. SPIE* **4841** (2003).
- [6] Modigliani, A., Hummel, W., Abuter, R., Amico, P., Ballester, P., Davies, R., Dumas, C., Horrobin, M., Neeser, M., Kissler-Patig, M., Peron, M., Reunanen, J., Schreiber, J., and Szeifert, T., "The sinfoni pipeline," *arXiv:astro-ph/0701297* (2007).